OPEN ACCESS
IOP Publishing | International Atomic Energy Agency Nuclear Fusion
Nucl. Fusion **55** (2015) 063021 (10pp) doi:10.1088/0029-5515/55/6/063021

Beryllium migration in JET ITER-like wall plasmas

S. Brezinsek[1], A. Widdowson[2], M. Mayer[3], V. Philipps[1], P. Baron-Wiechec[2], J.W. Coenen[1], K. Heinola[4], A. Huber[1], J. Likonen[4], P. Petersson[5], M. Rubel[5], M.F. Stamp[2], D. Borodin[1], J.P. Coad[2], A.G. Carrasco[5], A. Kirschner[1], S. Krat[3], K. Krieger[3], B. Lipschultz[2], Ch. Linsmeier[1], G.F. Matthews[2], K. Schmid[3] and JET contributors[a]

EUROfusion Consortium, JET, Culham Science Centre, Abingdon OX14 3DB, UK
[1] Forschungszentrum Jülich GmbH, Institut für Energie- und Klimaforschung—Plasmaphysik, 52425 Jülich, Germany
[2] CCFE Fusion Association, Culham Science Centre, Abingdon OX14 3DB, UK
[3] Max-Planck-Institut für Plasmaphysik, D-85748 Garching, Germany
[4] TEKES, VTT, PO Box 1000, 02044 VTT, Espoo, Finland
[5] Royal Institute of Technology (KTH), Association VR, 100 44 Stockholm, Sweden

E-mail: s.brezinsek@fz-juelich.de

Received 19 December 2014, revised 23 March 2015
Accepted for publication 25 March 2015
Published 8 May 2015

Abstract

JET is used as a test bed for ITER, to investigate beryllium migration which connects the lifetime of first-wall components under erosion with tokamak safety, in relation to long-term fuel retention. The (i) limiter and the (ii) divertor configurations have been studied in JET-ILW (JET with a Be first wall and W divertor), and compared with those for the former JET-C (JET with carbon-based plasma-facing components (PFCs)). (i) For the limiter configuration, the Be gross erosion at the contact point was determined *in situ* by spectroscopy as between 4% (E_{in} = 35 eV) and more than 100%, caused by Be self-sputtering (E_{in} = 200 eV). Chemically assisted physical sputtering via BeD release has been identified to contribute to the effective Be sputtering yield, i.e. at E_{in} = 75 eV, erosion was enhanced by about 1/3 with respect to the bare physical sputtering case. An effective gross yield of 10% is on average representative for limiter plasma conditions, whereas a factor of 2 difference between the gross erosion and net erosion, determined by post-mortem analysis, was found. The primary impurity source in the limiter configuration in JET-ILW is only 25% higher (in weight) than that for the JET-C case. The main fraction of eroded Be stays within the main chamber. (ii) For the divertor configuration, neutral Be and BeD from physically and chemically assisted physical sputtering by charge exchange neutrals and residual ion flux at the recessed wall enter the plasma, ionize and are transported by scrape-off layer flows towards the inner divertor where significant net deposition takes place. The amount of Be eroded at the first wall (21 g) and the Be amount deposited in the inner divertor (28 g) are in fair agreement, though the balancing is as yet incomplete due to the limited analysis of PFCs. The primary impurity source in the JET-ILW is a factor of 5.3 less in comparison with that for JET-C, resulting in lower divertor material deposition, by more than one order of magnitude. Within the divertor, Be performs far fewer re-erosion and transport steps than C due to an energetic threshold for Be sputtering, and inhibits as a result of this the transport to the divertor floor and the pump duct entrance. The target plates in the JET-ILW inner divertor represent at the strike line a permanent net erosion zone, in contrast to the net deposition zone in JET-C with thick carbon deposits on the CFC (carbon-fibre composite) plates. The Be migration identified is consistent with the observed low long-term fuel retention and dust production with the JET-ILW.

Keywords: JET tokamak, beryllium, material migration, erosion, deposition, ITER

(Some figures may appear in colour only in the online journal)

1. Introduction

The understanding of material migration, and thus the process cycle of material erosion, transport and deposition, is one of the key issues for a successful and safe operation of the ITER tokamak and a future fusion reactor. This process

[a] See the appendix of Romanelli F *et al* 2014 *Proc. 25th IAEA Fusion Energy Conf. (Saint Petersburg, Russia)*

cycle is associated with the lifetime of the first-wall material components, the so-called plasma-facing components (PFCs), under erosion, and with the safety aspect in relation to long-term tritium retention. The latter is an issue both for current fusion devices and for ITER, dominated by the co-deposition of tritium with eroded material [1]. Most of the present knowledge is based on tokamaks with carbon-based first-wall materials, and information obtained *in situ* from optical spectroscopy during plasma operation and combined with detailed post-mortem analysis after extraction of PFCs. In the common understanding, the main chamber is identified as the primary erosion source and material is transported via scrape-off layer (SOL) flows in a normal magnetic field configuration, predominantly towards the inner divertor region where finite material deposition occurs [2]. In a subsequent multistep process, material transport to remote and inaccessible areas takes place, which led to the abandoning of carbon (C) as a plasma-facing material due to the unacceptably high fuel retention in co-deposited layers, and this inhibits the safe conditions for ITER [3]. The outer divertor, though a net erosion zone, plays only a minor role in the overall large material transport which can reach g levels of migrating material for typical current day devices. Predictions for ITER and fusion reactors are based on this physical understanding, and the appropriate material selection is done with the aid of plasma–wall interaction codes such as ERO [4] and WallDYN [5]. The exchange of PFCs, as in ASDEX Upgrade from graphite to tungsten [6], and recently in JET from the carbon-fibre composite to beryllium (Be main chamber) and tungsten (W divertor) [7] provides the ideal test bed on which to verify the physical assumptions. Indeed, both devices demonstrated a reduction in fuel retention and transport to remote areas, which underlined the fact that with carbon, chemical erosion at low or thermal impact energy (ions and neutrals) dominated the material migration cycle.

Details concerning the residual carbon content in the JET-ILW are described in section 2, and the beryllium erosion and transport in the limiter configuration are presented in section 3 and in the divertor configuration in section 4. The overall migration in JET-ILW, differences with respect to JET-C, and the physical mechanisms responsible for the vast reduction of migration, as well as the absence of net deposition in the inner divertor strike line area, are given in section 5. Brief conclusions drawn for ITER from JET and a summary (section 6) complete this contribution.

2. The residual C content in JET-ILW operational regimes

The C content in the plasma edge dropped after installation of the JET-ILW by about a factor 20 in the diverted plasma phase of discharges throughout the first year of operation (C28–C30, marked by red diamonds in figure 1(a)), and prior to the exchange of selected PFCs for post-mortem analysis [8]. Figure 1(a) describes statistically the C plasma edge content in the main chamber, visualized via C III line emission and normalized with respect to the edge electron density $n_{e,edge}$, for all JET-ILW plasma discharges and, as a reference, for discharges executed in the last JET-C campaigns. The data are recorded in the middle of the divertor phase of each discharge and temporally averaged over one second. Additionally, the statistical mean value of individual campaigns is given as a green bar in the logarithmic graph, to allow a comparison of longer periods. The spreading in the C level can be attributed to different plasma conditions and auxiliary power levels [30]. Steep and short duration reductions in the C levels are related to strong Be evaporations [37] applied for conditioning and physical studies.

Predominantly deuterium plasmas were executed and show a clear lower envelope in the C level. In contrast, phases with partial or full helium operation show a significant drop in the statistical C level and can be attributed to the absence of chemical erosion of carbon or carbon layers under He bombardment. As this behaviour can be seen both in JET-C and in JET-ILW, in a similar manner but with lower absolute value, it is most likely that a large fraction of residual C in the JET-ILW in the deuterium plasma is resulting from low energy neutral deuterium bombardment of residual carbon layers on recessed metallic surfaces (e.g. the Inconel vessel) or CFC tile back sides in remote areas.

However, apart from an initial clean-up phase, the plasma operation can be described as virtually carbon-free in the first year with an absolute core carbon concentration of $C_C \simeq 0.1\%$ [9], whereas the residual C from the clean-up is found predominantly in net deposition zones like the divertor floor [20]. This steep initial clean-up phase of the roughly first 500 Ohmic discharges after the ILW installation and the moderate reduction of the C level up to pulse number 82 000 has been documented by optical C II emission spectroscopy in the divertor legs [8], via the C content profile in material deposits on inner divertor mirrors [35], and via the percentage of deuterated methane in the plasma exhaust analysed by gas chromatography in the active gas handling system for a large number of gas balances [8].

The overall C level remained low and one order of magnitude below the values in JET-C in the second year of JET-ILW operation after the tile intervention, labelled as C31–C33 in figure 1(b) and marked by blue diamonds. However, it is notable that the statistical spread is increased in the second year of operation (C31–C33) which can to a large extent be attributed to more extensive plasma operation with the outer strike line positioned on W-coated CFC close to the outer pump-duct entrance. Moreover, to improve plasma performance, the gas injection rate was decreased and the auxiliary power increased in the second operational year, which induced larger transient heat and particle fluxes to the W-coated CFC target plates in edge localized modes (ELMs). In contrast, the magnetic configurations in C28–C30 were predominantly executed with the outer strike line on the bulk W outer divertor target plate, at higher fuelling rates and lower auxiliary power levels.

Monitoring discharges with identical plasma shape and operational parameters have been regularly executed to document the change of the impurity content, and thus primarily the residual C levels, and the migrating Be in the JET vessel by optical spectroscopy [8]. Figure 2 shows for the inner and outer divertors the flux ratio of C II at 515 nm, representing primarily the re-eroded/reflected C flux, to D_γ, representing the recycling flux, as well as the flux ratio of Be II at 527 nm, representing primarily the re-eroded/reflected

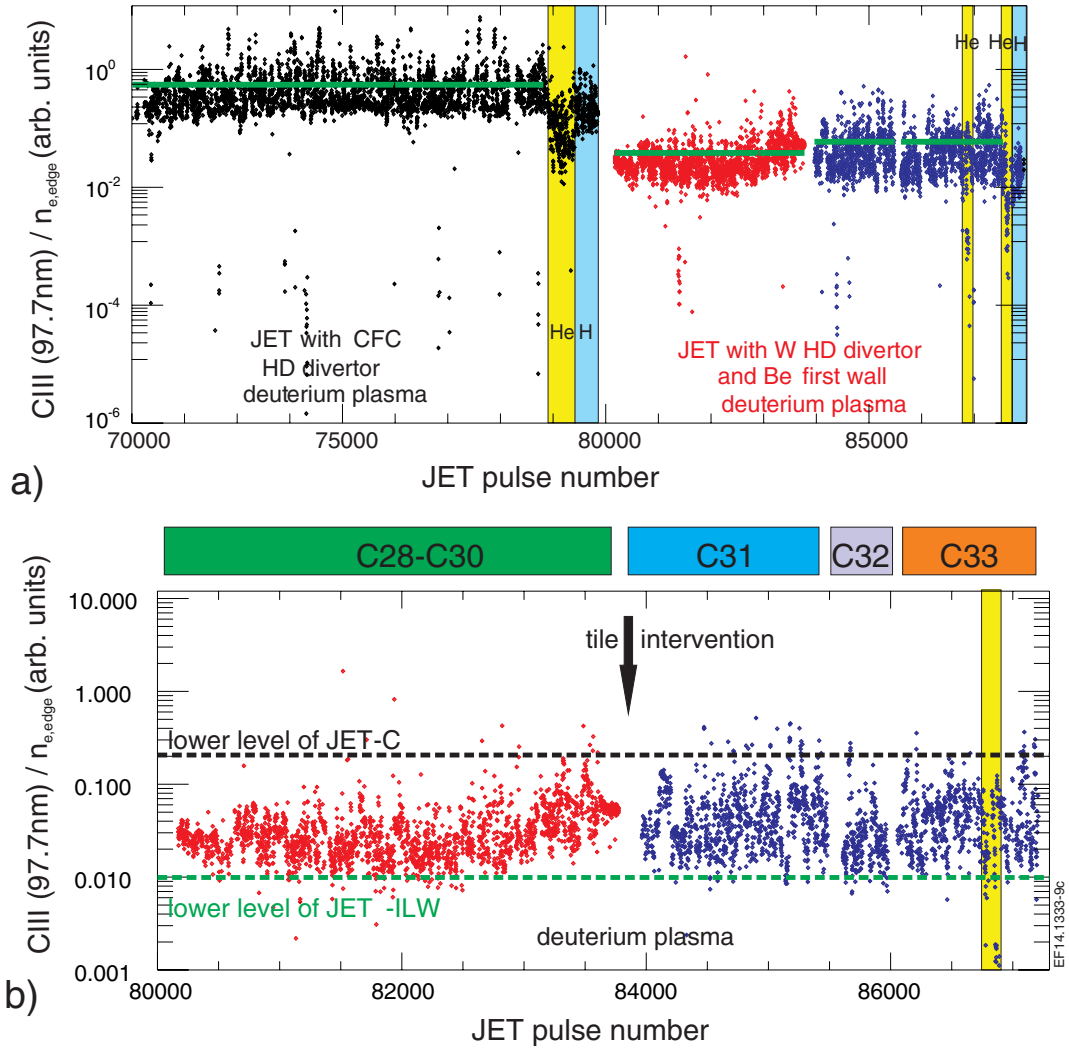

Figure 1. (a) Carbon contents (C II/$n_{e,edge}$) in the main chamber plasma edge in JET-C and JET-ILW during the divertor phase of the plasmas as a function of the discharge number between JPN 70 000 and 87 500. He-containing plasmas as well as hydrogen plasmas are indicated. (b) Enlarged view of the carbon content in the two years of JET-ILW operation. The lower envelope for the C content in JET-C and JET-ILW is marked as dashed lines. The period C28–C30 indicates the first year of operation followed by the tile intervention for post-mortem analysis. C31–C33 reflects the second year of JET-ILW operation.

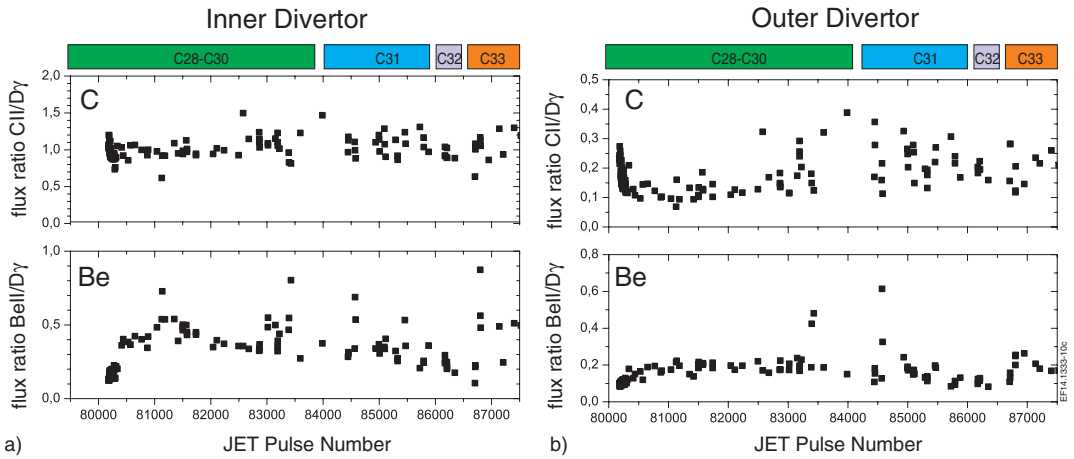

Figure 2. Development of the C (C II/D_γ flux ratio) and Be content (Be II/D_γ flux ratio) in the inner (a) and outer (b) legs in identical discharges spread of the full period of JET-ILW operation to monitor the Be and C evolution with time. The period C28–C30 indicates the first year of operation followed by the tile intervention for post-mortem analysis. C31–C33 reflects the second year of JET-ILW operation.

Be flux, to D_γ. The flux ratios give a good measure of the divertor impurity status, and the lower envelope in the case of C and the upper envelope in the case of Be reveal almost constant conditions in C and Be in the first year of operation after the previously mentioned initial C clean-up phase and a Be build-up phase [15]. Higher individual levels are attributed to conditioning issues for the vessel such as the first plasma after a long phase without operation etc [8]. However, a slight increase of the C content in the outer divertor of less than 50% in the period C33 with respect to the minimum C values in JET-ILW obtained in C28 has been detected and can be seen in both figures 2(a) and (b). The main reason for the long-term increase is the exposure of back faces of divertor CFC tiles which are not W coated by high neutral deuterium flux, by the release of C present *in situ* in the W coating of divertor PFCs due to the manufacturing process [34], and by C resulting from air leaks as well as, at high input power and low density operation, by potential damage of the W coatings. In particular, plasma shapes with the outer strike line positioned at the pump-duct entrance of the outer divertor, which shows enhanced plasma performance with respect to the confinement case [16], is connected to an increased C content from both the C embedded in the W coating itself and the C eroded at the back faces of the lower vertical target plate due to chemical erosion by low energy neutrals. The released C remains to a large extent in the system, which is reflected in the increase of the C content in the series of monitoring pulses; these pulses have been recorded since C28, with the outer strike line positioned on the bulk W divertor target plate and not on the W-coated one. Figure 2(a) shows also that at the end of the second year of operation a slight reduction of the Be base level in the inner divertor took place, which is probably a consequence of plasma operation at higher divertor electron temperatures in high performance H-mode plasmas prior to the execution of these standard monitoring discharges. The increase in the Be level at the beginning of C33 was attributed to a period with partial He operation in otherwise pure deuterium plasmas. The subsequent monitoring pulse documented the increase of the Be content in the plasma with respect to the reference values of preceding campaigns. The higher Be content is a consequence of the higher mass of He with respect to D in the physical sputtering process. Note that all post-mortem results presented here are from the first tile intervention following the operational period of constant divertor impurity conditions (C28–C30) where all W-coated CFC divertor tiles were intact; thus JET-ILW was presenting ultimately a tokamak with Be/W PFCs—a good test bed for ITER [9].

However, JET with its inertially cooled PFCs and the inductively pulsed operation is limited in discharge duration; the typical ratio between operational times in limiter and divertor configurations per discharge is about 1:3. Moreover, in the initial JET-ILW exploitation (2011–2012) a significant portion of the total plasma time (19 h) was devoted to limiter operation (6 h), which can be compared with 33 h plasma time in the divertor configuration and 12 h in the limiter configuration in the last JET-C operation period (2008–2009) [10]. Separation of the two operational regimes is required in order to describe the material migration cycle in JET-ILW by means of optical spectroscopy and post-mortem analysis of components.

3. Limiter configuration operation with the JET-ILW

JET operation in the limiter configuration was conducted to validate the design of the castellated massive Be PFCs, and to determine the Be sputtering yield, and through this, to verify the ERO code and available atomic and surface data; ERO has already been applied for obtaining lifetime predictions for first-wall Be components in ITER [26]. The local plasma conditions at the inboard limiters as well as the deuteron impact energies were varied in the range between 35 eV and 200 eV by deuterium fuelling in a series of inner-wall limited discharges dedicated to determining the effective Be sputtering yield. This effective yield for Be gross erosion at the limiter contact point was measured *in situ* by optical emission spectroscopy, observing Be II and D_γ, and determined as between 4.0%, predominantly due to deuteron impact, and more than 100%, predominantly due to Be self-sputtering (figure 3(a)) [12]. The measured yields are effective, as they are averaged over the observation chord at the limiter contact point which compromises the variation of impinging fluxes, impact angles, surface temperatures and plasma conditions. Therefore, these effective Be yields were compared with ERO calculations considering these variations and providing synthesized diagnostic views to benchmark the code and its input data directly with the spectroscopic measurements. ERO calculations overestimate the effective Be yield by about a factor of 2, which can be partially attributed to shadowing effects of neighbour inner wall limiters [11].

The effective Be erosion yields are also about a factor of 2 larger than effective C erosion yields in JET-C, whereas the contribution of self-sputtering of C at the high impact energy end is smaller. At the accessible low impact energy end of these limiter discharges, the yield of Be is lower than that of C, though chemically assisted physical sputtering (CAPS) of Be via BeD has been identified as contributing to the total effective Be sputtering yield, as shown in figure 3(b). At an impact energy of 75 eV and $T_{\mathrm{Be_{base}}} = 200\,^{\circ}\mathrm{C}$ the erosion is enhanced by 1/3 with respect to the normal physical sputtering case [12]. $T_{\mathrm{Be_{base}}}$ is the quasi-equilibrium plasma-facing component temperature before the plasma discharge to which the actual temperature increase due to the plasma load ($\Delta T = 80\,^{\circ}\mathrm{C}$) needs to be added to provide the actual Be surface temperature ($T_{\mathrm{Be_{surface}}} = 280\,^{\circ}\mathrm{C}$) at the time of the spectroscopic measurement [12]. CAPS acts as an additional sputtering channel, but requires a certain amount of deuterium to be present on the topmost Be interaction layer, which can reach a fuel content of 50% as calculated using SDTrimSP in [36]. As the deuterium content decreases with the surface temperature, this being caused by desorption [15], the impact of CAPS on the total Be sputtering yield decreases with the surface temperature and vanishes at $T_{\mathrm{Be_{base}}} \geqslant 520\,^{\circ}\mathrm{C}$. The BeD released can be in the form of BeD_x with $x = 1, 2, 3$, whereas only BeD was experimentally observed by optical emission spectroscopy in JET. With increase of $T_{\mathrm{Be_{base}}}$, D_2 is directly desorbed from the Be surface, reducing the deuterium content in the interaction layer and causing a decrease of BeD emission, whereas the deuterium recycling flux remained constant [12]. Indeed, the contribution of CAPS to the total effective Be sputtering yield observed in JET at $E_{\mathrm{in}} = 75$ eV is in line with experimental results from PISCES-B [27], where CAPS

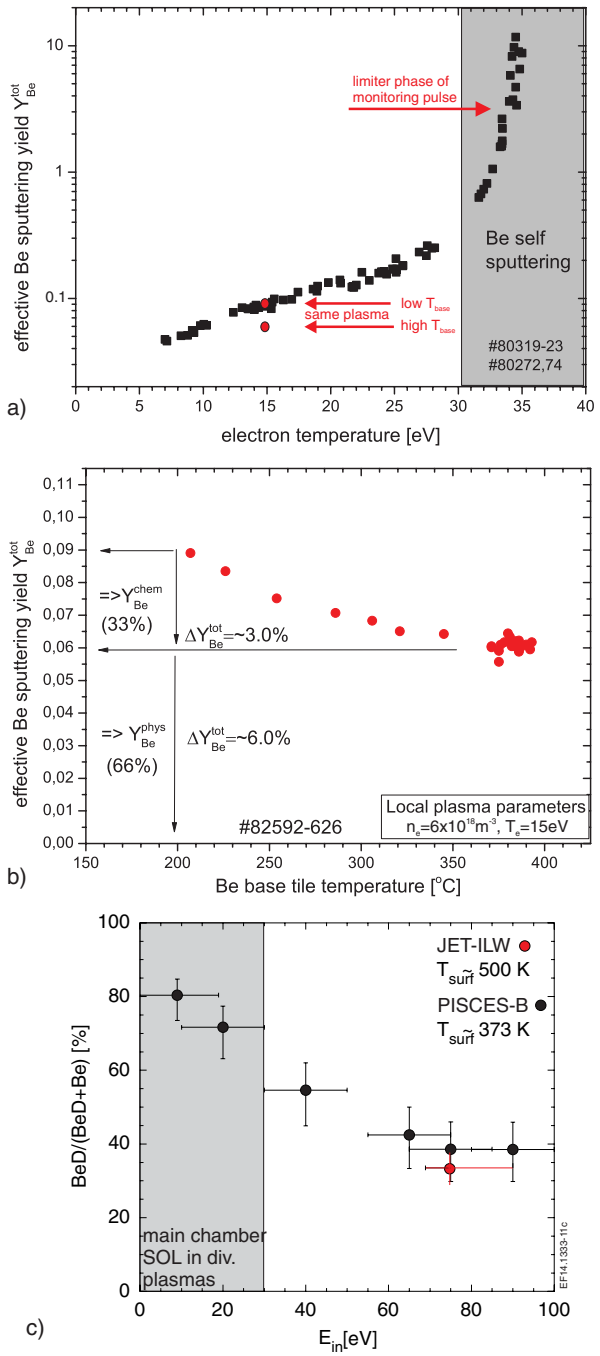

Figure 3. (a) The effective Be sputtering as a function of the electron temperature, proportional to the impact energy of the impinging ions at almost constant surface temperature. The effective sputtering is determined by the deuterons at the lower energy range and the Be ions at the higher energy end (shadowed area). (b) Composition of the effective Be sputtering yield as a function of surface temperature at constant impact energies in a series of identical discharges. (c) The normalized contribution of chemically assisted physical sputtering of Be to the total effective Be sputtering yield as a function of the impact energies for deuterium ions in PISCES-B and JET-ILW.

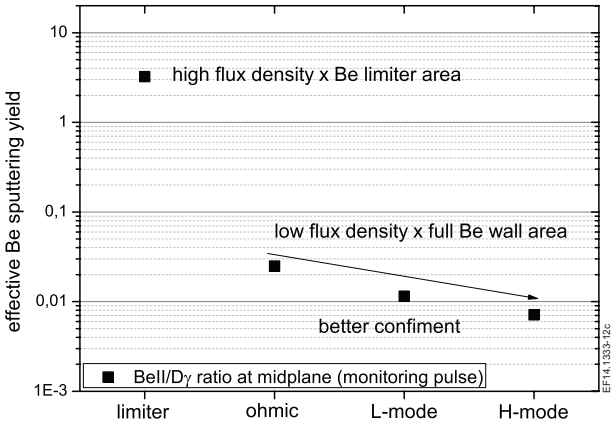

Figure 4. Typical effective Be sputtering yields in different operational phases (limiter, Ohmic, L mode and H mode).

was identified before and studied as a function of the biasing and temperature at the Be target plate. Figure 3(c) shows the contribution of CAPS to the total effective Be sputtering yield in PISCES-B and JET as a function of the impact energy. The molecular dynamics approach can reproduce the fraction of Be erosion sputtered via CAPS [28], but this is not yet in agreement with the surface temperature dependence observed in JET. The implementation of CAPS as an erosion process in ERO is currently ongoing and will increase the confidence in the ITER predictions concerning the Be PFC lifetime. It should be noted that CAPS gains importance over classical physical sputtering at low impact energies (figure 3(c)); however, as the process is physically driven, a minimum impact energy is required for sputtering the Be, which is greatly in contrast with the case for chemical erosion of C, where even thermal deuterons or neutrals can induce chemical erosion via methane etc [29].

In a first approximation, deduced from spectroscopic measurements of Be II, and thus Be^+, which is unaffected by the initial beryllium sputtering process, an effective Be gross erosion yield of 10% can be estimated to be the representative yield for the averaged limiter plasma conditions in the initial JET-ILW campaign. The averaging includes limiter plasma discharges as well as the limiter start-up phases in diverted plasmas weighted with respect to the operational time at a given central density or, better, impact energy. This results in an averaged limiter plasma representative for the campaign, whose impact energy can be used to determine the effective yield according to figure 3. This averaging includes also cases of self-sputtering, as are present in the limiter phase of monitoring discharges (figure 4) or the limiter phase of the first diverted plasmas executed with the JET-ILW [15]. It should be noted that from the campaign C29 on, the deuterium injection rate during the limiter start-up phase has been raised in order to increase the plasma electron density and decrease the electron temperature, which inhibits significant Be self-sputtering during the limiter start-up phase. This averaged yield for the limiter phase converts to an average gross Be erosion rate of 4.1×10^{18} Be s^{-1} or 1.5 g Be sputtered from one limiter tile ($A_{tile} = 0.025$ m^2) in the view of the spectroscopic system (the observation chord marked in figure 5(a) with $A_{spot} = 0.011$ m^2) in the first year. Post-mortem analysis of Be tiles of inboard limiters (figure 5(b)) extracted after the first year of operation provides information on the campaign-averaged Be erosion rate from different techniques (profilometry, nuclear reaction analysis (NRA), Rutherford backscattering spectrometry (RBS)) [10, 13, 14].

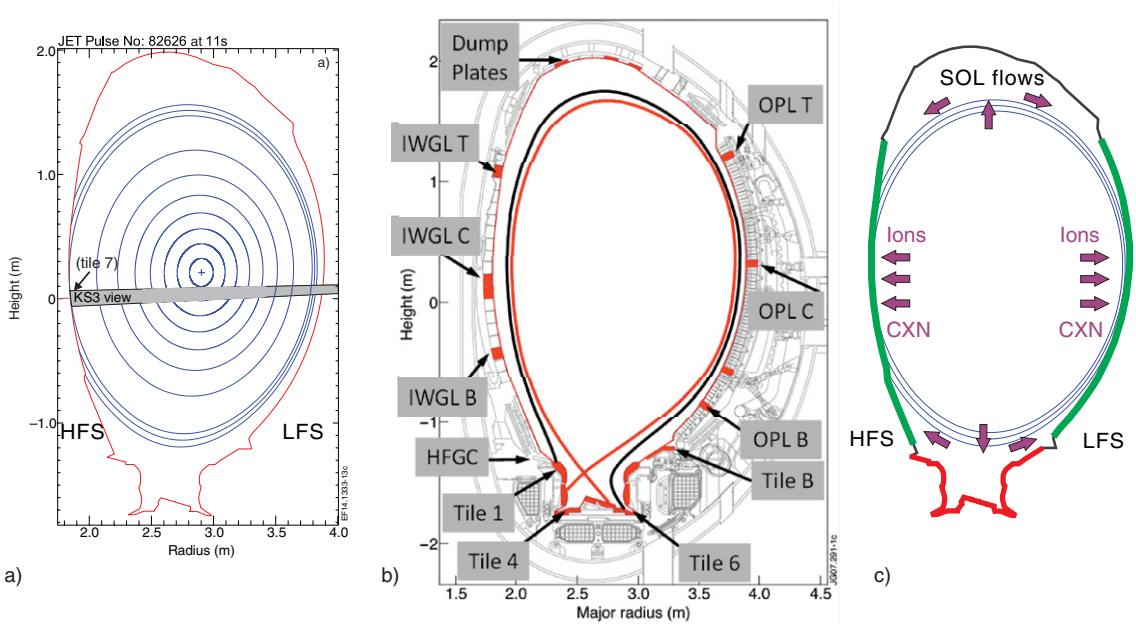

Figure 5. (a) Spectroscopic observation chord spotting on the inner wall at the contact point in the limited plasmas applied. (b) Poloidal cross-section of JET with plasma-facing components extracted and analysed by post-mortem techniques, in red. (c) Be migration path in limited plasmas without Be transport into the W divertor.

The net erosion rate for one midplane Be tile amounts to 2.3×10^{18} Be s^{-1} if one considers the normalization with respect to the total limiter exposure time in the campaign. This is equivalent to 0.8 g Be net erosion from one midplane tile, which can be compared with spectroscopy findings, resulting in a factor of 2 between the net erosion and gross erosion.

Comparison of the net erosion with the corresponding tile in JET-C and normalization with respect to the operational time reveals a higher erosion rate in the JET-ILW case; however, taking into account the different numbers of interacting limiters in JET-C (#16) and JET-ILW (#10) reduces the discrepancy. The primary impurity source in the limiter configuration in JET-ILW is only 25% greater than that for the JET-C case. This is in good agreement with the spectroscopic observations, considering that some erosion of the limiters also takes place in the diverted plasma phase and that gross versus net erosion is compared.

For the total Be source estimation, both spectroscopy and post-mortem analysis must extrapolate the local information to the total limiter interaction area, which represents a fraction of the total inner wall protruding limiters ($A_{\rm lim}^{\rm HFS} = 4.5$ m^2). Additional measurements on the top and bottom tiles of the high field side (HFS) poloidal limiter rail were obtained, showing the peak erosion in the centre and almost negligible erosion in the other areas. Interpolation in the poloidal direction and extrapolation to all inner wall toroidal limiters results in an estimation of the total Be gross erosion of about 12 g in the first year of ILW operation. Apart from in dedicated experiments, limiter operation is required in the ramp-up and ramp-down phases in all JET-ILW discharges connecting plasmas to the HFS and low-field side (LFS) limiters. Post-mortem analysis revealed that the erosion on the LFS limiters is poloidally asymmetric [13] with stronger erosion at the lower half of the limiter rail with the maximum at the centre. This centre tile showed Be erosion of at least 10 μm—erasing an Ni marker layer, which challenges absolute quantification on the LFS.

The main fraction of Be eroded at the limiters in the limiter configuration stays within the main chamber (figure 5(c)), mostly deposited in recessed areas like the limiter wings and partially on the wall cladding; only a small fraction of neutral Be escapes geometrically from the main chamber into the divertor entrance, and can be deposited there. Indeed the initial JET-ILW experiment in the diverted configuration identified moderate surface coverage of W by Be [15] after 625 s in the limiter configuration. However, the amount entering the divertor is insignificant in comparison with the Be transported into the divertor in X-point plasmas with strike lines positioned on the target plates.

4. Divertor configuration operation with the JET-ILW

With the full W divertor installed in the JET-ILW, no PFCs made of the main chamber wall material are used in the divertor; thus, all Be ions flowing into the divertor are originated primarily in the main chamber during diverted plasma operation. Figure 4 shows the change in the effective Be sputtering yield in the main chamber during the different phases of the monitoring discharge mentioned before and described in [30]: the limiter phase, Ohmic divertor phase, L-mode phase and H-mode phase. The effective Be sputtering yield drops strongly due the fact that (a) the limiter phase is in the Be self-sputtering regime, (b) the impact energy of impinging ions drops from the limiter phase to the divertor phase due to the cold SOL plasma, and (c) the confinement of the particles in the plasma increases. The total Be source can be estimated by appropriate multiplication with the Be surface interaction area as described below. Almost homogenous Be and BeD emission in toroidal and poloidal directions at the inner wall midplane can be observed by spectroscopy using

different lines of sight on the cladding area and the limiters which are both representing recessed areas. The origin of the erosion processes in these recessed areas is twofold: energetic charge exchange neutrals (CXN) and residual plasma flux are impinging on the recessed HFS wall area ($A_{\rm wall}^{\rm HFS} = 18.5$ m^2). The inner wall is covered primarily with Be-coated Inconel cladding tiles ($A_{\rm clad}^{\rm HFS} = 11.2$ m^2, of which 2/3 are Be and the rest protective W tiles) separated by the poloidal Be limiters ($A_{\rm limiters}^{\rm HFS} = 7.3$ m^2) which are located in the radial direction typically between 6 cm and 10 cm behind the separatrix. Horizontal movement of the plasma column by several cm, and thus variation of the distance to the Be surface of the same degree, is causing variations of the Be and BeD flux, indicating that the low energy deuterium ion flux contributes significantly to the erosion of the Be cladding.

Dedicated Be long-term samples (sachet samples) installed at different poloidal and toroidal locations between the cladding tiles prior to the first ILW plasma being present were replaced after the first year of operation for post-mortem analysis. All probes show measurable erosion [17], confirming that the Be cladding is a zone of net erosion, as do the limiters which are about 2 cm closer to the plasma, but still deep in the SOL. Quantification of the erosion was performed by using RBS, providing a local Be erosion rate of 0.78×10^{18} Be m^{-2} s^{-1} when normalized with respect to the total operational time. This results in a net erosion of 12.2 g of Be from the whole inner wall in the integrated divertor time of the first ILW campaign. This rate can be directly compared with the erosion rate of 3.14×10^{19} C m^{-2} s^{-1} obtained in the 2005–2009 operational phase in JET-C, where similar long-term samples were installed and analysed [18]. This is a significant difference, by a factor of 4.0. The ratio between the total sputtering yields of Be and C gets even larger and amounts to 5.3 when the different total area of CFC cladding in JET-C, as compared to the Be cladding in JET-ILW, is considered. The CXN fluxes and the residual plasma flux impinging on the first wall are similar in the two JET PFC configurations; a difference in the erosion processes involved is required to explain the difference in the primary impurity source. Indeed this difference can be explained solely by chemical erosion of C at the lowest, even thermal, impinging energies of deuterium. Though CAPS in the case of Be has been observed, the process is different to the thermally activated chemical erosion of C, as a clear energetic threshold at about 10 eV energy exists [33] which inhibits the erosion below this minimum required damage energy. The reduction of the impurity concentration in the plasma edge and the primary erosion source is also consistent with the reduction of the C content observed in JET-C in He plasmas. In both cases—the JET-ILW case with D plasma and the JET-C case with He plasma—the fundamental process of chemical erosion at low impact energies is absent and this can explain the drop in the impurity content which is then reflected in the corresponding values of $Z_{\rm eff}$ in the plasma core ($Z_{\rm eff} = 1.2$ in JET-ILW D plasma, $Z_{\rm eff} = 2.5$ in JET-C He plasma and $Z_{\rm eff} = 2.0$ in JET-C in D plasma) [9].

The total main chamber Be source in the diverted configuration includes also Be eroded from the low field side. However, in contrast to the high field side case, no outer wall Be cladding exists which can be bombarded with CXN and residual plasma flux. The space between the poloidal limiters is filled with large ports for heating systems (e.g. heating by neutral beams), diagnostics (e.g. VUV diagnostics), and blank areas of the Inconel vessel. Thus, the outer wall Be source in the diverted configuration is determined by the poloidal limiters which are typically 4–8 cm away from the separatrix, closer than the inner wall cladding. The measured erosion of limiters, mentioned in the previous section, is partially caused by CXN, by residual plasma flux and, potentially, by enhanced filamentary transport [19]. An exact quantification of the outer wall Be source is therefore currently not possible, but a lower estimate can be obtained by assuming the same erosion rate as on the inboard Be cladding over the total outer limiter area ($A_{\rm lim}^{\rm LFS} = 9$ m^2) assuming at least similar CXN and residual plasma flux to the inner and outer SOL and ignoring the filamentary transport responsible for the asymmetry. The lower estimate for the total net main chamber source in the diverted configuration amounts to $\simeq$21.2 g.

It should also be noted that the long-term samples in the recessed areas are measuring a net erosion which in the above calculation is assumed to be the result of a static process. But it cannot be excluded that the net erosion may result from a dynamic process where in certain operational periods material is deposited also, but then more strongly re-eroded in other periods, depending on the ion and CXN flux impinging on the sample location. By this dynamic mechanism, the actual throughput of Be material can be enhanced. Indeed the emission of Be light from recessed W-coated tiles located on the high field side of the main chamber indicates that this path of deposition/re-erosion exists, but it cannot yet be quantified, and this is a task for further studies when more tile analysis is available to close the balance. Moreover, the contribution of erosion from the damaged upper dump plate during diverted plasma operation has not been considered. However, initial post-mortem analysis suggests that the contribution from this location is small [14] which is greatly in contrast with the JET-C case, where the upper dump plate was a strong primary erosion source. Furthermore, Be erosion has been observed on protection tiles and protection limiters (e.g. for RF antennae) which need to be taken into the Be source calculation in future when post-mortem analysis results are available. All three corrections will lead to an increase of the primary erosion source of Be in the diverted configuration with the JET-ILW; however, the total erosion source strength will remain substantially lower than that of the C source in JET-C.

5. Overall material migration with the JET-ILW

The current understanding of the material migration in the JET-ILW in the divertor configuration can be described as follows (figure 6(a)): neutral Be and BeD are eroded by physical sputtering and CAPS, respectively, from the recessed main chamber wall equipped with Be PFCs. Both Be and BeD enter the plasma, dissociate in the case of the molecule, ionize and are transported by SOL flows towards the inner divertor where significant deposition of Be on W PFCs takes place. Indeed post-mortem analysis revealed that the majority of all deposition is found on top of the apron of the inner divertor (on the HFGC (high field gap closure) tile and tile 1 in figure 5(b)) which are, in all diverted plasmas, located

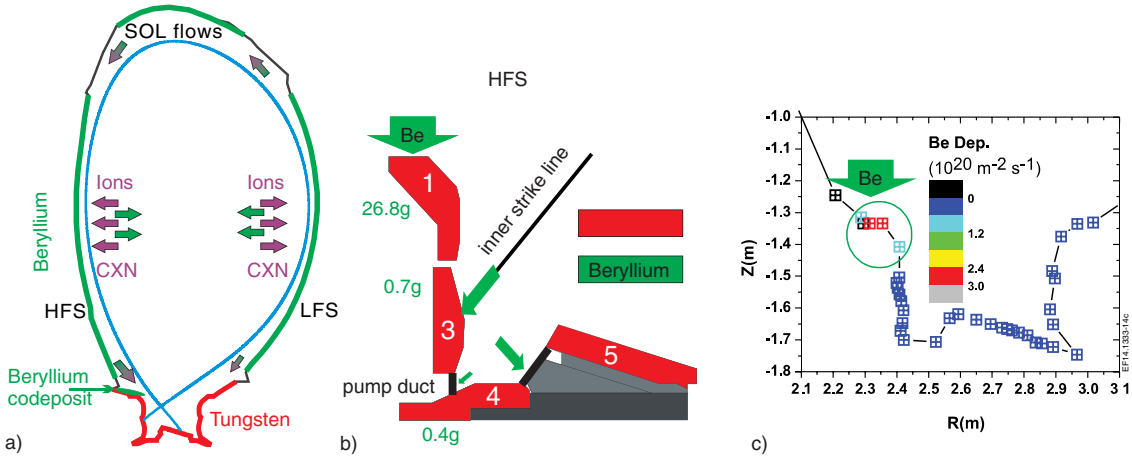

Figure 6. (a) Beryllium migration path in the diverted plasma configuration: from the Be main chamber into the W divertor. (b) Material migration within the inner divertor leg; the Be deposition distribution in g on the inner divertor PFCs. (c) WallDYN modelling of an H-mode divertor discharge, which shows qualitatively the observed experimental deposition pattern on top of tile 1 [21].

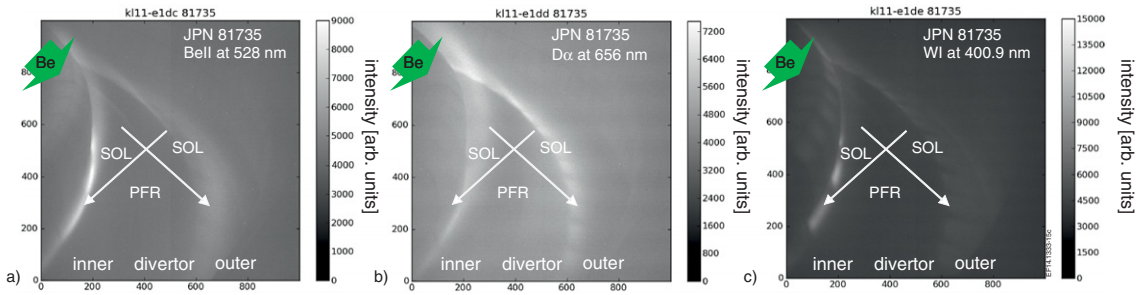

Figure 7. Emission of (a) Be II and (b) D_α in the divertor during a quiet L-mode phase. The inner and outer strike lines are visible. (c) W I light emission in the inner divertor leg showing no W I at the top of tile 1 where Be deposits and strong W I along the vertical target with a maximum near the inner strike line location. The strong emission at the strike line indicates an intact W surface and no coverage with Be deposit.

in the far SOL [20]. The total deposition at this location of cold surface temperature (T_{surf} 373 K) amounts to at least 28 g. This marks the first net deposition location of material driven by SOL flow (figure 6(b)), and indeed the WallDYN code can reproduce this observation well, as depicted in figure 6(c). The process of migration in the main chamber described might proceed in several steps, as suggested by the diagonal form of the redistribution matrix in WallDYN [21]. The observed net deposition location for Be depends on the local balance of the erosion and the deposition flux. Details of the WallDYN code and the benchmark with JET gas balance results [1] and the post-mortem deposition pattern [10] can be found in [21]. Further transport from this apron location is strongly hindered, as the local plasma conditions do not provide enough energetic deuterons to re-erode the deposited Be; thus the majority of Be just sticks and builds up a Be layer which incorporates the majority of the retained fuel. This is different to the JET-C and C cases, where chemical erosion and multiple-step transport with ten or more re-erosion cycles occurred, which moved the deposited C along the vertical target plate down to the pump duct entrance, resulting in a strong net deposition zone of the whole inner divertor target plate in JET-C [10].

The inner strike line is for the majority of diverted plasmas in the first year of JET-ILW operation located on the vertical target (tile 3) as shown in figure 6(b). The incident Be ion flux is not sufficient to turn this area into a Be net deposition zone, but reflection and energetic sputtering by deuterons and impurities in steady-state conditions and in particular during ELMs take place [9, 22, 24]. As no Be deposition layer is built up, the W-coated CFC vertical tiles 1 and 3, close to the campaign-averaged strike line position, are indeed representing a net W erosion zone as *in situ* W I spectroscopy revealed and recent post-mortem analysis confirmed [22]. Figure 7 shows e.g. the emission pattern of (a) Be II at 527.1 nm, (b) D_α, and (c) W I at 400.9 nm in the full W divertor, recorded simultaneously in the L-mode phase of a monitoring discharge after about 1500 plasma discharges since the first plasma with the JET-ILW. The strong W I line emission at the inner strike line and along the vertical W target plate is clearly visible, indicating that the area is not covered by a Be deposited layer. The W I emission is peaked close to the PFC surface due to the short penetration depth of neutral W in the attached inner and outer divertor legs, which is similar to observations made using TEXTOR [31]. However, on the PFCs made of W-coated CFC, islands with Be deposition can also be identified in the W net erosion areas, which can be attributed to the large surface roughness of the coatings. This is analogous to observations made for ASDEX Upgrade equipped with W PFCs and impacted by C impurities [32].

Overall, the Be transport to the divertor floor and, to an even greater extent, that to the remote area of the pump duct entrance are strongly reduced (by a factor of 50) with respect

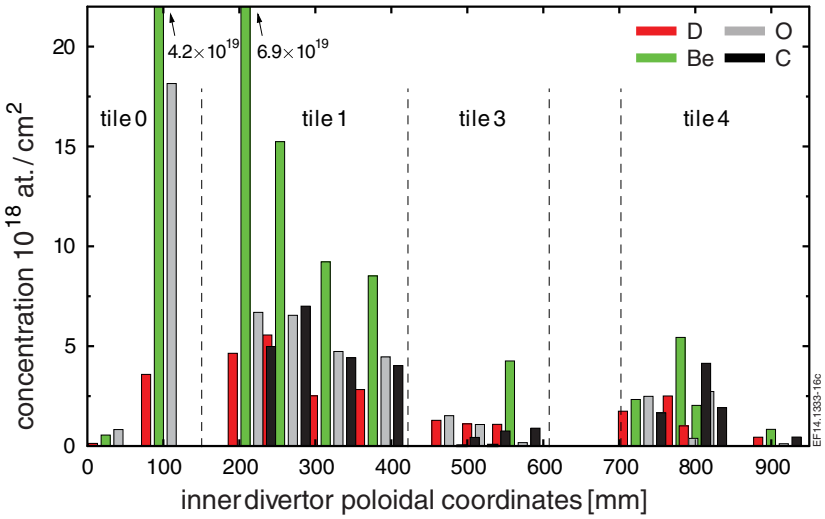

Figure 8. Beryllium deposition in the inner divertor leg determined post-mortem by ion beam techniques, from [13]. Additionally, the impurities carbon and oxygen, as well as deuterium, are shown in the bars.

to that for C in JET-C, as measurements and associated ERO modelling confirmed [23]. In the case of JET-C, chemical erosion of C was responsible for the multistep transport which is vastly reduced for Be in the JET-ILW due to the energetic threshold for Be sputtering inhibiting re-erosion by low energy particles such as thermal neutrals. Detailed post-mortem analysis of the residual impurity composition of the W surface in the inner leg reveals [22] the spatial C and O impurity distribution [25] as depicted in figure 8. The fraction of O and C with respect to Be is enhanced on the horizontal target plate 4 with respect to the vertical target plates and, in particular, with respect to the Be deposition on the apron which shows high Be purity. It can be concluded that C is re-eroded and enriched at the divertor floor like in JET-C due to chemical erosion, but at orders of magnitude lower areal densities.

The outer divertor shows a completely different erosion/deposition pattern with respect to the inner divertor leg. Though a poloidal SOL flow from the outer wall SOL, starting at the stagnation point, down into the outer leg exists, the amount of Be ions arriving in the outer divertor is insufficient to cause net deposition on top of tile 8. Also the vertical target plates (tile 7 and tile 8) are not affected and show no sign of erosion or significant deposition. Note that the outer strike line was in the first year of operation predominantly positioned on the bulk W divertor (tile 5 in figure 7(b)), which partially explains the virgin-like conditions of the vertical W target plates. Tile 5 has not yet been analysed post-mortem, but *in situ* W sputtering from the incident Be ion flux was observed and it can be assumed that the W surface is clean and free from impurities, deposits or discolourations—almost pristine [9].

6. Summary

JET equipped with a Be first wall is an ideal test bed for ITER, for studying beryllium erosion and migration paths as well as verifying plasma–surface interaction codes such as ERO and WallDYN. Benchmarking of the ERO code was done in dedicated limiter discharges, determining spectroscopically the beryllium erosion at the inner wall limiters. Besides the ordinary physical sputtering, chemically assisted physically sputtering was also identified and the total erosion determined. Beryllium eroded in these discharges is predominantly redistributed in the main chamber of JET and only a small fraction can escape geometrically into the divertor. WallDYN was applied to verify this global migration behaviour in the limiter configuration.

In the divertor configuration, the amount of beryllium eroded in the main chamber (cladding and limiters) is about 21 g and the amount of beryllium deposited in the inner divertor is comparable, amounting to 28 g in the first year of JET-ILW operation—considering the currently analysed PFCs and assuming a static main chamber source. This fairly good balance confirms the main understanding of the beryllium migration processes in the diverted configuration and the beryllium transport in the SOL towards the inner divertor. WallDYN calculations confirm the migration behaviour and can simultaneously reproduce the final deposition area of beryllium and match at the same time the long-term fuel retention. The absence of chemical erosion in the case of beryllium inhibits the multistep transport (via deposition/erosion steps) seen with carbon and JET-C. This avoids the re-erosion of beryllium deposited on the apron of the inner divertor tungsten PFCs and its transport to remote areas, and further the accumulation of beryllium in inaccessible areas in the pump ducts or below, as observed with carbon in JET-C. Beryllium sticks in less than two interaction steps to the tungsten PFCs, as ERO divertor simulations [23] and divertor deposition monitors [24] indicate.

The primary impurity source in the diverted configuration for the JET-ILW is significantly reduced in comparison with the JET-C case, resulting in a reduction in divertor material deposition by more than an order of magnitude [20]. The absence of low energy sputtering of beryllium is responsible for the reduction of the primary source in JET-ILW with respect to JET-C, where the erosion of carbon PFCs by thermal neutrals contributed to the source production. The overall low beryllium migration is also consistent with the observed low fuel inventory and dust production with the JET-ILW [9]. However, more divertor and main chamber PFCs need to be analysed before a full balance can be achieved.

Acknowledgments

This work was carried out within the framework of the EUROfusion Consortium and has received funding from the European Union's Horizon 2020 research and innovation programme under grant agreement number 633053. The views and opinions expressed herein do not necessarily reflect those of the European Commission.

References

[1] Brezinsek S. *et al* 2013 *Nucl. Fusion* **53** 083023
[2] Pitts R.A. *et al* 2005 *Plasma Phys. Control. Fusion* **47** B303
[3] Roth J. *et al* 2009 *J. Nucl. Mater.* **390–1** 1
[4] Kirschner A. *et al* 2000 *Nucl. Fusion* **40** 989
[5] Schmid K. 2011 *et al J. Nucl. Mater.* **415** S284
[6] Neu R. *et al* 2013 *J. Nucl. Mater.* **438** S34
[7] Matthews G.F. *et al* 2013 *J. Nucl. Mater.* **438** S1
[8] Brezinsek S. *et al* 2013 *J. Nucl. Mater.* **438** S303
[9] Brezinsek S. *et al J. Nucl. Mater.* in press (doi:10.1016/j.jnucmat.2014.12.007)
[10] Widdowson A. *et al* 2014 *Phys. Scr.* T **159** 014010
[11] Borodin D. *et al* 2014 *Phys. Scr.* T **159** 014057
[12] Brezinsek S. *et al* 2014 *Nucl. Fusion* **54** 103001
[13] Heinola K. *et al J. Nucl. Mater.* in press (doi:10.1016/j.jnucmat.2014.12.98)
[14] Baron-Wiechec A. *et al J. Nucl. Mater.* in press (doi:10.1016/j.jnucmat.2015.01.058)
[15] Krieger K. *et al* 2013 *J. Nucl. Mater.* **438** S262
[16] Joffrin E. *et al* 2015 *Nucl. Fusion* submitted
[17] Krat S. *et al* 2015 *J. Nucl. Mater.* **456** 106
[18] Mayer M. *et al* 2013 *J. Nucl. Mater.* **438** S780
[19] Carallero D. *et al J. Nucl. Mater.* in press (doi:10.1016/j.jnucmat.2014.10.019)
[20] Rubel M. *et al* 2015 *Nucl. Fusion* submitted
[21] Schmid K. *et al* 2015 *Nucl. Fusion* submitted
[22] Mayer M. *et al* 2015 *PFMC Conf. (Aix-en-Provence, May 2015)*; *Phys. Scr.* submitted
[23] Kirschner A. *et al J. Nucl. Mater.* in press (doi:10.1016/j.jnucmat.2014.10.072)
[24] Beal J. *et al J. Nucl. Mater.* in press (doi:10.1016/j.jnucmat.2014.09.069)
[25] Petersson P. *et al J. Nucl. Mater.*in press (doi:10.1016/j.jnucmat.2014.12.077)
[26] Borodin D. *et al* 2011 *Phys. Scr.* T **145** 14008
[27] Nishijima D. *et al* 2008 *Plasma Phys. Control. Fusion* **50** 125007
[28] Björkas C. *et al* 2009 *New J. Phys.* **11** 123017
[29] Roth J. *et al* 1996 *Nucl. Fusion* **36** 1647
[30] Coenen J.W. *et al* 2013 *Nucl. Fusion* **53** 073043
[31] Brezinsek S. *et al* 2011 *Phys. Scr.* T **145** 014016
[32] Schmid K. *et al* 2010 *Nucl. Fusion* **50** 105004
[33] Björkas C. *et al* 2013 *Plasma Phys. Control. Fusion* **55** 074004
[34] Ruset C. *et al* 2009 *Fusion Eng. Des.* **84** 1662
[35] Ivanova D. *et al* 2014 *Phys. Scr.* T **159** 014011
[36] Borodin D. *et al* 2013 *J. Nucl. Mater.* **438** S267
[37] Brezinsek S. *et al* 2011 *Nucl. Fusion* **51** 073007